Crystal structure of phospholipase PA2-Vb, a protease-activated receptor agonist from the Trimeresurus stejnegeri snake venom

ARTICLE *in* FEBS LETTERS · NOVEMBER 2014

Impact Factor: 3.17 · DOI: 10.1016/j.febslet.2014.10.032

6 AUTHORS, INCLUDING:

Maikun Teng

University of Science and Technology of Ch…

134 PUBLICATIONS **1,512** CITATIONS

SEE PROFILE

Xu Li

University of Science and Technology of Ch…

58 PUBLICATIONS **362** CITATIONS

SEE PROFILE

Bing Shen

Anhui Medical University

35 PUBLICATIONS **525** CITATIONS

SEE PROFILE

FEBS Letters xxx (2014) xxx–xxx

journal homepage: www.FEBSLetters.org

Crystal structure of phospholipase PA2-Vb, a protease-activated receptor agonist from the *Trimeresurus stejnegeri* snake venom

Fuxing Zeng [a,1], Wenjuan Zhang [a], Nairui Xue [b], Maikun Teng [a], Xu Li [a,*], Bing Shen [b,*]

[a] Hefei National Laboratory for Physical Sciences at Microscale and School of Life Sciences, University of Science and Technology of China, Hefei, Anhui 230026, People's Republic of China

[b] Department of Physiology, Anhui Medical University, Hefei, Anhui 230032, People's Republic of China

ARTICLE INFO

Article history:
Received 10 August 2014
Revised 7 October 2014
Accepted 27 October 2014
Available online xxxx

Edited by Christian Griesinger

Keywords:
Acidic phospholipase A_2
Vasoconstrictor activity
Ca^{2+} release
IP_3 receptor
Crystal structure

ABSTRACT

Phospholipase A_2 (PLA_2) is an important component in snake venoms. Here, an acidic PLA_2, designated PA2-Vb was isolated from the *Trimeresurus stejnegeri* snake venom. PA2-Vb acts on a protease-activated receptor (PAR-1) to evoke Ca^{2+} release through the inositol 1,4,5-trisphosphate receptor (IP_3R) and induces mouse aorta contraction. PAR-1, phospholipase C and IP_3R inhibitors suppressed PA2-Vb-induced aorta contraction. The crystal structure reveals that PA2-Vb has the typical fold of most snake venom PLA_2. Several PEG molecules bond to a positively charged pocket. The finding offers a novel pharmacological basis of the structure for investigating the PAR-1 receptor and suggests potential applications for PA2-Vb in the vascular system.

1. Introduction

Snake venom exhibits a variety of toxic effects including neurotoxicity, cardiotoxicity and myotoxicity. By means of toxic effects, snakes can survive in complex environments [23,26,28,34]. Phospholipase A_2 (PLA_2) is commonly found in snake venoms as well as mammalian tissues. Functionally, PLA_2 specifically recognizes the sn-2 acyl bond of phospholipids and catalytically hydrolyzes the bond to release arachidonic acid and lysophospholipids involved in many critical biological processes [14,30]. In snake venom, PLA_2 ($svPLA_2$) also inhibits A-type K^+ currents in rat dorsal root ganglion neurons [12]. Several crystal structure studies suggest that most $svPLA_2$s share a common set of structural features, including their small molecular mass (14–18 kDa) and a compact structure with seven conserved disulfide bonds and an important Ca^{2+}-loop [21].

Calcium ion signals in vascular smooth muscle cells (VSMCs) include Ca^{2+} flashes, oscillations, puffs, ripples, sparkletts, sparks, waves and rises in the global intracellular Ca^{2+} level ($[Ca^{2+}]_i$) [3,40]. The sources of Ca^{2+} ions are mainly from extracellular Ca^{2+} entry and intracellular Ca^{2+} store release. In vascular smooth muscle cells (VSMCs), the primary intracellular Ca^{2+} store is sarcoplasmic reticulum (SR) [36]. Two common Ca^{2+} release channels, the inositol 1,4,5-trisphosphate receptor (IP_3R) and the ryanodine receptor (RyR), are located in the SR membrane [8]. It is well known that numerous G-protein coupled receptors (GPCRs), including protease-activated receptor (PAR-1), link to IP_3R-mediated Ca^{2+} release, resulting in a rise in VSMC $[Ca^{2+}]_i$ and vasoconstriction [11]. IP_3R regulates VSMC contractility, gene expression, migration and proliferation by modulating their intracellular Ca^{2+} homeostasis. Several diseases, including hypertension, atherosclerosis and diabetes-related vascular complications, are linked to the malfunction of IP_3R and the consequent changes in Ca^{2+} signaling [24].

The present study describes the purification and structural characteristics of an acidic PLA2, named PA2-Vb, which was iso-

Abbreviations: PLA_2, phospholipases A_2; PAR-1, protease-activated receptor 1; IP_3R, inositol 1,4,5-trisphosphate receptor; $svPLA_2$, snake venom PLA_2; VSMCs, vascular smooth muscle cells; SR, sarcoplasmic reticulum; RyR, ryanodine receptor; GPCRs, G-protein coupled receptors; RP, reversible permeabilization; *p*BPB, *p*-bromofenacil bromide; 2-APB, 2-aminoethoxy diphenyl borate; PLCβ, phospholipase Cβ

* Corresponding authors at: Room 412, School of Life Sciences, University of Science and Technology of China, Hefei, Anhui 230026, People's Republic of China (X. Li). Fax: +86 551 65161132 (B. Shen).

E-mail addresses: sachem@ustc.edu.cn (X. Li), shenbing@ahmu.edu.cn (B. Shen).

[1] Present address: Department of Biochemistry, University of Illinois at Urbana-Champaign, 600 S Mathews Ave, 493 Roger Adams Laboratory, Urbana, IL 61801, USA.

http://dx.doi.org/10.1016/j.febslet.2014.10.032
0014-5793/

lated from *Trimeresurus stejnegeri* snake venom, as well as its PAR-1-mediated Ca^{2+} releasing effect.

2. Materials and methods

2.1. Purification of PA2-Vb

PA2-Vb was purified from the lyophilized crude venom of *T. stejnegeri* (Tunxi Snakebite Institute, Anhui, China) by a three-step chromatographic procedure at 14 °C as previously described [38]. The detailed methods are described in the supplementary material.

2.2. Enzymatic assays

The enzymatic activity of PA2-Vb was determined using a turbidimetric method with egg yolk phospholipids as a substrate [13]. One egg yolk was suspended in 1 L of physiological saline and 0.2 ml of the suspension was mixed with 0.8 ml 0.1 M Tris, pH 8.0. Then, 0.1 mg of PA2-Vb was added and the mixture was incubated at 30 °C. The decrease in the suspension turbidity was monitored, and the absorbance was recorded at 740 nm. One unit was defined as the amount of enzyme that produced a decrease of 0.01 in absorbance in 10 min. The specific activity was expressed as U/mg.

2.3. Isolation of the thoracic aorta and tension measurements

All animal experiments were conducted in accordance with NIH publication No. 8523 and were approved by the Institutional Animals Care and Use Committee of Anhui Medical University. The isolated aortic rings for tension measurements were prepared as previously described [39]. The detailed method is described in the supplementary material.

2.4. Reversible permeabilization

Heparin was loaded into the cell using a reversible permeabilization (RP) method [15]. The detailed method is described in the supplementary material.

2.5. Modification by pBPB

His^{48} in PLA_2 was modified by *p*-Bromophenacyl Bromide (*p*BPB) using a protein to reagent molar ratio of 1:5 [20]. At room temperature, PA2-Vb (1 mg) was dissolved in 1 ml 25 mM Tris, pH 8.0, and then 0.4 mM *p*BPB was added from a stock solution in acetone. When the residual activity was less than 1%, the reaction mixture was acidified to pH 3.0 to quench the reaction. The unbound *p*BPB was removed on a desalting column (GE Healthcare). The *p*BPB-conjugated PA2-Vb was then applied to the vessel for tension measurements and enzymatic assays.

2.6. VSMC primary culture and $[Ca^{2+}]_i$ measurement

Under a dissecting microscope, the endothelium-denuded aortic strips were placed in an ice-cold PBS solution (137 mM NaCl, 2.7 mM KCl, 10 mM Na_2HPO_4, 2 mM KH_2PO_4, pH 7.4) and cut into small blocks (2 × 2 mm) [25]. These tissue blocks were then pasted on the bottom of cell culture dishes and cultured in DMEM in a 37 °C incubator. After 4–7 days, VSMCs gradually grew out from the edge of the vessel tissues.

For the $[Ca^{2+}]_i$ measurement, the primary cultured VSMCs were loaded with 10 μM Fluo-8/AM and 0.02% F-127 for 60 min in the dark at 37 °C in an NPSS (140 mM NaCl, 5 mM KCl, 1 mM $CaCl_2$, 10 mM glucose and 5 mM HEPES, pH 7.4 with NaOH). After three washes with a Ca^{2+}-free NPSS solution, the fluorescence signal of the VSMCs was measured by a confocal laser scanning microscope (ZEISS 710, objective EC Plan-Neofluar 10×/0.30 M27). The wavelength of the excitation laser light was 488 nm. The $[Ca^{2+}]_i$ rise was displayed as a ratio of fluorescence intensity relative to that induced by ATP application (F/F_{ATP}).

2.7. Crystallization and data collection

The PA2-Vb was concentrated to 20 mg/ml in 5 mM Tris, 50 mM NaCl, pH 7.5. Crystallization screens were performed at 14 °C by the hanging-drop vapor-diffusion method with 1 μl protein solution and 1 μl reservoir solution. Hampton Research Crystal Screens were used to screen for crystallization conditions. After one week, high quality rod-shaped crystals appeared in a drop containing 12% PEG8000, 0.1 M sodium phosphate, pH 6.5 and were obtained for data collection. A diffraction data set was collected at 100 K with cryoprotectant solution (reservoir solution supplemented with an additional 20% (v/v) glycerol) using MAR345 image plate on beamline BL17U at the Shanghai Synchrotron Radiation Facility (SSRF) and was processed to 1.60 Å using HKL2000 [18].

2.8. Model building, sequence determination and refinement of the crystal structure

The phase of the PA2-Vb crystal was solved by molecular replacement using Molrep [31] from the CCP4 package [19] using the structure of the PLA_2 from *Agkistrodon piscivorus* venom (PDB entry: 1VAP) as the search model [10]. The model completion was performed in COOT [7] and the refinement was performed using REFMAC5 [17]. Using the homologous protein sequences, the amino acid sequence of PA2-Vb was determined in accordance with the electron density map. For structurally similar amino acids, we corrected the side chains by comparing the homologous sequences to the shape of the F_O–F_C map. The R-factor and free R-factor of the final refined model are 18.3% and 20.9%, respectively. The overall assessment of model quality was checked by MolProbity [4] and PROCHECK [16]. The atomic coordinates have been deposited in the Protein Data Bank with accession code 4RFP. Detailed information about data collection and processing are presented in Table 1. Figures were prepared using PyMOL (DeLano Scientific LLC).

2.9. Incubation with heparin

The effect of heparin on the enzymatic activity of PA2-Vb was determined by pre-incubating the PLA_2 with heparin (2.5 μg/μg of enzyme) for 30 min at 25 °C followed by the activity assay.

2.10. Statistical analysis

Results are expressed as the mean values ± the standard deviation (mean ± SD). Statistical analysis between two independent samples was performed with the student's *t*-test. The significance was considered at a level of $P < 0.05$. In the concentration-response curves, the data were fitted to the sigmoidal dose-response equation with a variable Hill slope using Origin software.

3. Results

3.1. Purification of PA2-Vb and enzymatic characterization

PA2-Vb was isolated from *T. stejnegeri* venom by a three-step chromatographic process (Fig. 1). The SDS–PAGE profile of PA2-Vb shows a single band of ~14 kDa under non-reducing conditions

Please cite this article in press as: Zeng, F., et al. Crystal structure of phospholipase PA2-Vb, a protease-activated receptor agonist from the *Trimeresurus stejnegeri* snake venom. FEBS Lett. (2014), http://dx.doi.org/10.1016/j.febslet.2014.10.032

Table 1
Data collection and refinement statistics for PA2-Vb.

Data collection	
Resolution (Å)	50.0–1.60 (1.63–1.60)[a]
Wavelength (Å)	0.97915
Oscillation width (deg)	1
Exposure time (s)	1
Space group	$P2_12_12$
Unit cell parameters (Å)	a = 72.18, b = 85.71, c = 38.89
No. of unique reflections	32 661 (1659)[a]
Redundancy	11.0 (11.4)[a]
Completeness (%)	98.7 (100)[a]
Average I/σ (I)	10.9 (7.5)[a]
R_{merge}[b] (%)	16.6 (44.5)[a]
Refinement	
Resolution (Å)	36.85–1.60
No. of reflections for refinement/test	30970/1643
R_{work}[c] (%)/R_{free}[d] (%)	18.3/20.9
Rmsd for bonds (Å)	0.0084
Rmsd for angles (deg)	1.278
Mean B factor (Å^2)	24.25
No. of water oxygen atoms	187
Ramachandran plot (%)	
Most favored regions	91.3
Additional allowed regions	7.7
Generously allowed regions	1.0

[a] Values in parentheses are for the highest-resolution shell.
[b] $R_{merge} = \sum|I_i - \langle I\rangle|/\sum|I|$, where I_i is the intensity of an individual reflection and <I> is the average intensity of that reflection.
[c] $R_{work} = \sum||F_o| - |F_c||/\sum|F_o|$, where F_o and F_c are the observed and calculated structure factors for reflections, respectively.
[d] R_{free} was calculated as R_{work} using the 5% of reflections that were selected randomly and omitted from refinement.

(insertion in Fig. 1c). To confirm the purity, PA2-Vb was loaded onto a C18 reverse-phase HPLC column, which showed PA2-Vb appearing as a single major peak (Fig. 1d), indicating that the purity of PA2-Vb was high enough to be used in the subsequent experiments. As a member of the phospholipase, its enzymatic activity was tested and the result indicates that PA2-Vb efficiently cleaved egg yolk phospholipids with a specific enzymatic activity of $6.8 \pm 0.3 \times 10^4$ U/mg (n = 4 independent measurements, Fig. 2). Conversely, the enzymatic activity of PA2-Vb was strongly inhibited by the treatment with *p*BPB (Fig. 2). After the incubation of PA2-Vb with heparin, a slight increase in enzymatic activity was observed (Fig. 2), which is similar to other snake PLA_2s [27].

3.2. Effect of PA2-Vb on vasoconstriction and Ca^{2+} mobilization in VSMCs

When snakes attack human beings, the venom is injected into the human body. The venom diffuses into the circulatory system and alters blood vessel tension. Therefore, we tested the effect of PA2-Vb on the vasoconstriction. Endothelium-denuded mouse aortic rings were pre-contracted in a high concentration K^+ solution. After 15 min, 500 nM PA2-Vb was added into the bath. Interestingly, PA2-Vb further contracted the vessel rings with an EC_{50} of 86 nM (n = 5, the Hill slope is 1.49 ± 0.14, Fig. 3a and b). Because PA2-Vb is a phospholipase A_2, we used *p*BPB to block its enzymatic activity. However, the data show that *p*BPB conjugation did not alter its effect on the vasoconstriction following the high K^+-induced contraction (Fig. 3d). In another set of experiments, 500 nM PA2-Vb transiently constricted the vessel rings in the absence of high K^+ solution (6.1 ± 1.4% of high K^+-induced constriction, n = 5, Fig. 3c).

Calcium ions are a primary factor for triggering muscle cell contraction. In VSMCs, an L-type Ca^{2+} channel is the main pathway for mediating extracellular Ca^{2+} influx. Thus, we used 2 μM nifedipine to inhibit L-type Ca^{2+} channels or omitted extracellular Ca^{2+} ions (Ca^{2+}-free) to eliminate extracellular Ca^{2+} influx. However, the results show that PA2-Vb was still able to induce a transient vasoconstriction without significant inhibition (Fig. 3e). In addition to the extracellular Ca^{2+} influx, cytosolic Ca^{2+} also comes from Ca^{2+} stores that are released by IP_3R and/or RyR. We utilized ryanodine to block RyR and used 2-aminoethoxy diphenyl borate (2-APB) and

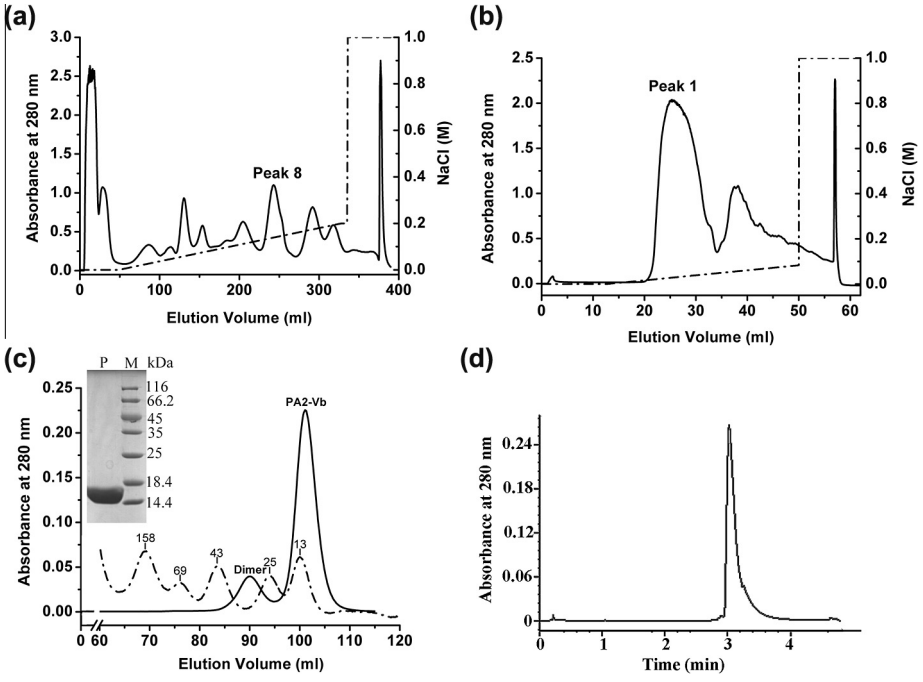

Fig. 1. Purification of PA2-Vb from *T. stejnegeri* venom. (a and b) Q XL and Mono Q chromatography. (c) Superdex 200 size-exclusion chromatography. The dashed line and numbers indicate the elution markers (in kDa). The inset shows the SDS–PAGE gel image. Lane P, PA2-Vb; lane M, molecular mass markers (in kDa). (d) HPLC chromatography.

Please cite this article in press as: Zeng, F., et al. Crystal structure of phospholipase PA2-Vb, a protease-activated receptor agonist from the *Trimeresurus stejnegeri* snake venom. FEBS Lett. (2014), http://dx.doi.org/10.1016/j.febslet.2014.10.032

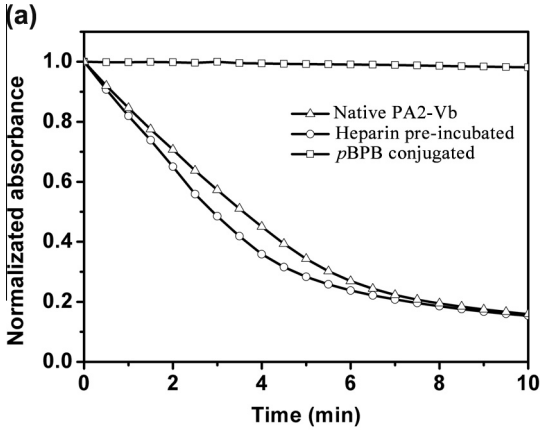

(b)

	Enzymatic activity (U/mg)
Native PA2-Vb	$6.8 \pm 0.3 \times 10^4$
Heparin pre-incubated	$8.0 \pm 1.1 \times 10^4$
*p*BPB conjugated	inhibited

Fig. 2. The effect of the native, heparin pre-incubated and *p*BPB conjugated PA2-Vb on egg yolk phospholipids.

heparin to inhibit IP_3R. We observed that ryanodine did not inhibit PA2-Vb-induced vasoconstriction; however, 2-APB and heparin significantly abolished PA2-Vb-induced vasoconstriction. This result suggests that PA2-Vb-induced vasoconstriction may be affected by IP_3R-mediated Ca^{2+} release. Therefore, to further investigate the mechanism, the SR Ca^{2+} pump inhibitor thapsigargin was used to deplete the Ca^{2+} stores. The data indicate that PA2-Vb-induced vasoconstriction disappeared upon thapsigargin treatment (Fig. 3e).

Because PA2-Vb is a macromolecule that is too large to transport into VSMCs, PA2-Vb-induced IP_3R activity may be through GPCRs-mediated Ca^{2+} signaling. We used U73122 to inhibit phospholipase Cβ (PLCβ) which is downstream of GPCRs. The result shows that U73122 abolished PA2-Vb-induced vasocontraction (Fig. 3e). Interestingly, we also found that the protease activated receptor-1 (PAR-1) inhibitor SCH79797 significantly blocked the PA2-Vb-induced vasocontraction (Fig. 3e).

To clarify the role of Ca^{2+} in the PA2-Vb-induced vasocontraction, intracellular Ca^{2+} levels were measured. In the primary culture VSMCs, 500 nM PA2-Vb evoked a transient $[Ca^{2+}]_i$ rise (Fig. 4), while 2-APB dramatically abolished the PA2-Vb-induced rise in $[Ca^{2+}]_i$ (Fig. 4b and c).

3.3. Sequence and structural features of PA2-Vb

Using homologous sequences and the high resolution (1.6 Å) of the data, the amino acid sequence in the PA2-Vb structure was determined based on the electron density map (Fig. 5). To show the quality of the structure, the electron density maps of the representative regions including the Ca^{2+}-loop and C-loop are presented in Fig. 5a and b. The sequence of PA2-Vb has high homology to

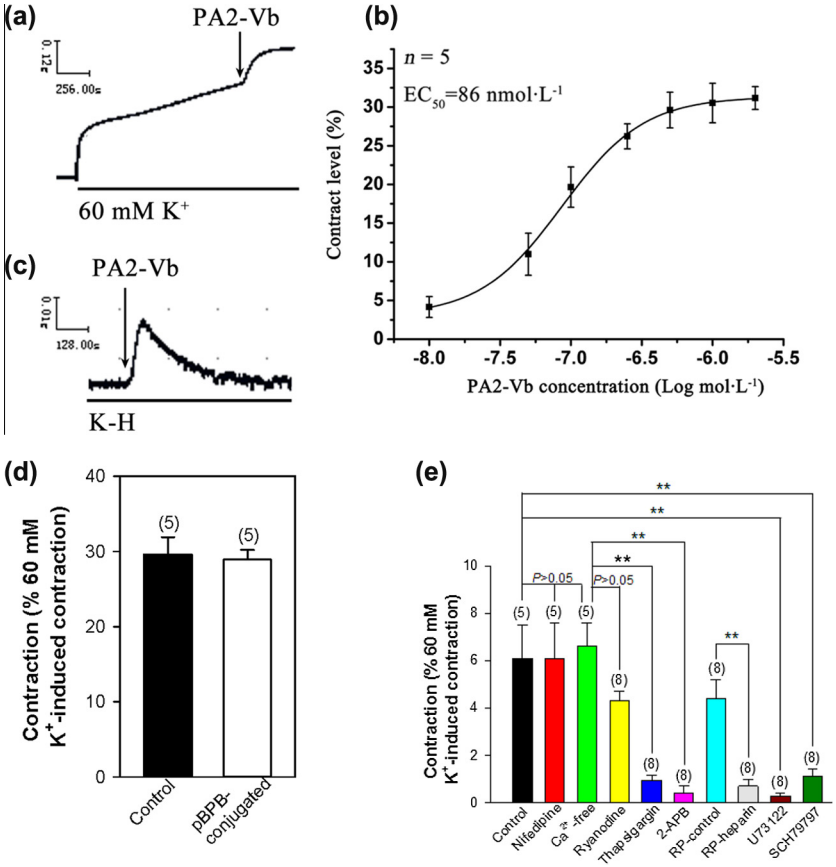

Fig. 3. The contractile effect of PA2-Vb on mouse thoracic aortic rings. (a) Contractile response induced by 500 nM PA2-Vb following 60 mM K^+-induced contraction. (b) Concentration-response curve for the contractile effect. (c) Contractile response induced by 500 nM PA2-Vb in normal Krebs Henseleit solution. (d) Summary of the data showing the *p*BPB effect on PA2-Vb-induced vasocontraction after 60 mM K^+-induced contraction. (e) Summary of the data showing the PA2-Vb-induced vasocontraction in the presence of different inhibitors and Ca^{2+}-free assays. RP: reversible permeabilization. K–H: Krebs Henseleit solution. Results are the mean ± S.D. (n = 5 or 8 independent experiments). $^{**}P < 0.01$ compared with the corresponding control group.

Please cite this article in press as: Zeng, F., et al. Crystal structure of phospholipase PA2-Vb, a protease-activated receptor agonist from the *Trimeresurus stejnegeri* snake venom. FEBS Lett. (2014), http://dx.doi.org/10.1016/j.febslet.2014.10.032

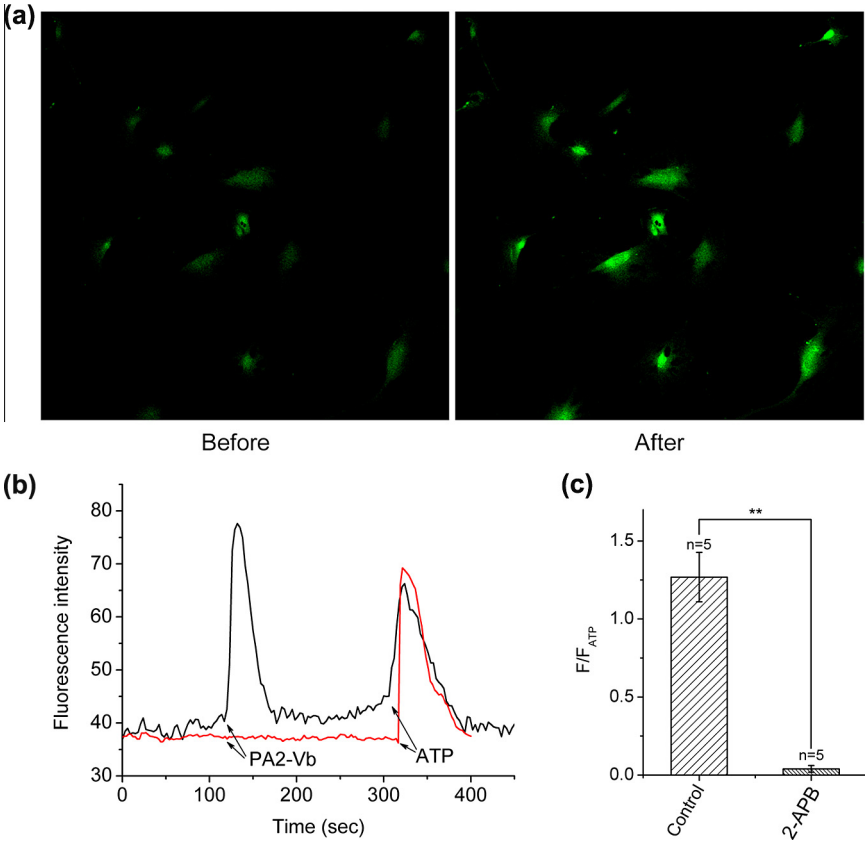

Fig. 4. PA2-Vb-induced intracellular Ca^{2+} ($[Ca^{2+}]_i$) rise in vascular smooth muscle cells (VSMCs): (a) Representative fluorescence images of primary cultured VSMCs before (*left*) and after (*right*) 500 nM PA2-Vb treatment. (b and c) Representative traces and summarized data of $[Ca^{2+}]_i$ rise induced by 500 nM PA2-Vb in primary cultured VSMCs. Results are the mean ± S.D. (n = 5 independent experiments). $^{**}P < 0.01$ compared with the control group.

other svPLA$_2$s. Only five residues are different between PA2-Vb and PA2-V, which is also isolated from *T. stejnegeri* snake venom (Fig. 5c).

The overall structure of PA2-Vb displays the typical fold of a svPLA$_2$ (Fig. 6a). The crystal has two molecules in the asymmetric unit. Superposition of the C_α atoms of the two monomers yields an RMSD of 0.69 Å, indicating the similarity of the two molecules (A and B). In Protein Data Bank, more than one hundred of structures of svPLA$_2$ (or complex) have been solved. Using the molecular A of PA2-Vb as a search model, DALI search [11] showed that PA2-Vb has a highly conserved structure to other svPLA$_2$s for example 1.0 Å RMSD and 69% sequence identity against 1IJL, an acidic PLA$_2$ from the venom of Deinagkistrodon acutus [9] and 1.1 Å RMSD and 69% identity against 1VAP [10]. Similar to other svPLA$_2$s, PA2-Vb has seven disulfide bridges in each monomer with and six canonical features (Figs. 5c and 6a): (i) an N-terminal α-helix (H1), (ii) a 'short' helix (η1), (iii) a Ca^{2+}-binding loop, (iv) two anti-parallel α-helices (H2 and H3), (v) two short strands of anti-parallel β-sheet (β-wing), and (vi) a C-terminal loop. In the crystal structure, four PEG molecules were observed. One of them is located in the pocket formed by residues Ala^{13}/Arg^{16}/Trp^{21}/Lys^{110}/Tyr^{113}/Arg^{114} in monomer A (Fig. 6b). The other three PEG molecules are located in the same pocket in monomer B (Fig. 6c). All four of the PEG molecules interact with residues in PA2-Vb through many hydrogen bonds and hydrophobic interactions.

3.4. Oligomeric assembly

The results of Superdex 200 chromatography indicate that PA2-Vb is predominantly in a monomer in solution. But a significant homodimer peak was also observed (Fig. 1c). The SDS–PAGE analysis of PA2-Vb under non-reducing conditions showed a single band for the monomer (insertion of Fig. 1c). This indicates that the homodimer in the solution is not formed by disulfide bond. Meanwhile, the crystal structure shows a homodimer, which is stabilized by the interactions in two sites (Fig. 7). Interactions in site one (S1) mainly consist of hydrogen bonds between Lys^{31} in monomer A and Asp^{49}/Phe^{28} in monomer B (Fig. 7a, c and d). Site two (S2) includes several hydrophobic interactions in the 60-loop, H1 helix, Ca^{2+}-loop and C-loop (Fig. 7b–d). S2 comprises the interface-binding surface (i-face) of the PLA$_2$. The examination of the crystal unit-cell packing using the PISA software shows a complete buried interface of 1582.3 Å^2 (12.6% of the total surface area), and $\Delta^i G = -7.6$ kcal/mol. The dimer in the structure is in a grey area of complexation criteria; it may or not be stable in the solution, which was consistent with the Superdex200 results.

4. Discussion

In this study, an acidic PLA$_2$ called as PA2-Vb was isolated from *T. stejnegeri* snake venom. The sequence alignment with other snake PLA$_2$s shows that PA2-Vb is an isoform of PLA2-V (Accession Number: P82896) which was also purified from *T. stejnegeri*. However, the biological characteristics of PLA2-V were largely unknown. Here we show that PA2-Vb has a strong vasoconstriction activity by acting on PAR-1.

In the vessel tension measurements, PA2-Vb was able to induce a contractile response, in both high K^+ and normal solutions. This vasoconstriction effect was also found in other snake toxins, such as natratoxin, a secreted PLA$_2$ from *Naja atra* venom which can effectively inhibit A-type K^+ currents [12] and AhV_TL-I, a thrombin-like enzyme from *A. halys pallas* which acts on RyRs to evoke

Please cite this article in press as: Zeng, F., et al. Crystal structure of phospholipase PA2-Vb, a protease-activated receptor agonist from the *Trimeresurus stejnegeri* snake venom. FEBS Lett. (2014), http://dx.doi.org/10.1016/j.febslet.2014.10.032

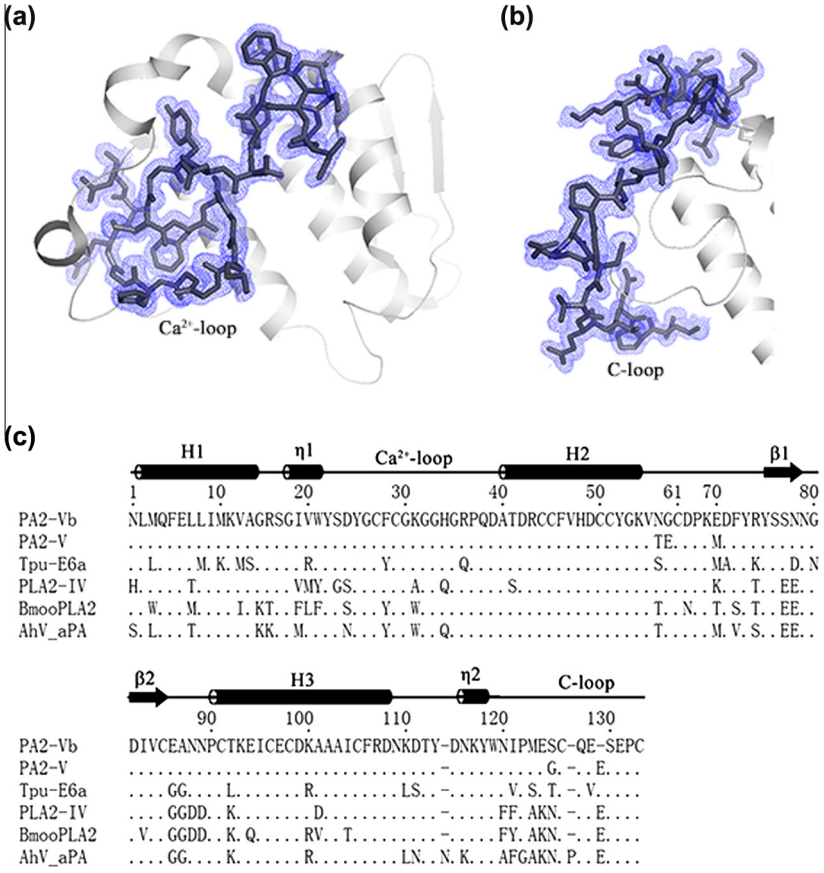

Fig. 5. Electron density maps and sequence alignment of PA2-Vb. (a and b) The electron density maps (2Fo-Fc, σ1.0) of the Ca^{2+}-loop and the C-loop, respectively. (c) Multiple alignments with other svPLA$_2$s.

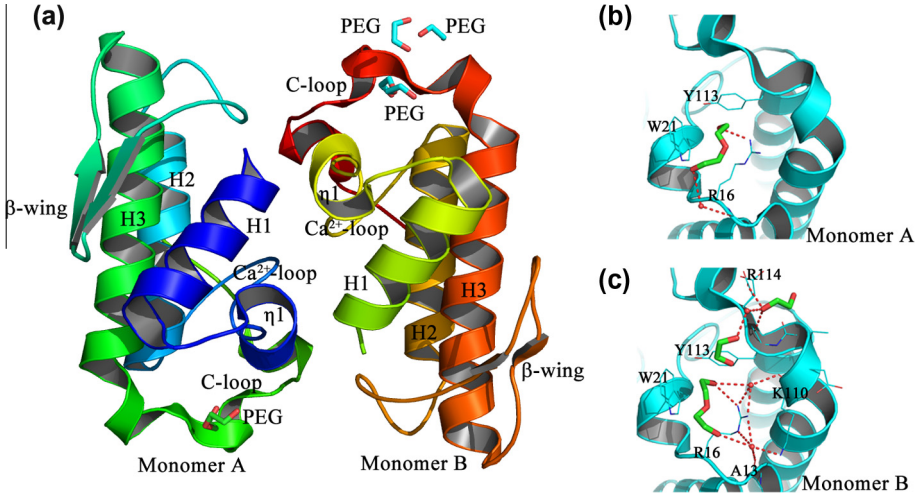

Fig. 6. Structure of PA2-Vb. (a) Ribbon representation of the PA2-Vb structure. (b and c) The PEG molecules in monomer (a) A and (b) B. The hydrogen bonds are shown in red dot lines. The interacting amino acids are shown as thin sticks and the PEG molecules are shown as bold green sticks. The red and blue in the sticks represent oxygen atoms and nitrogen atoms, respectively. The small red balls represent waters involved in the interaction.

Ca^{2+} release [37]. In this study, the results show that the intracellular Ca^{2+} release mediated by IP_3R results in vasoconstriction. In addition, PAR-1 and PLCβ inhibitors both abolished the PA2-Vb-induced vasoconstriction. This line of evidence indicates that PA2-Vb might act on the PAR-1 receptor, leading to G protein activation. The subsequently activation of PLCβ to produce IP_3 then activates IP_3R to mediate Ca^{2+} release and muscle cell contraction. Therefore, we have not only uncovered the working mechanism underlying the PA2-Vb-induced vasoconstriction, but more importantly, we have identified the molecular target of the PA2-Vb toxin in the cells. In our previous study, AhV_TL-I was shown to indirectly activate RyR [37]. Meanwhile, PAR-1-PLCβ-IP_3R-mediated Ca^{2+} release is involved in the vasoconstriction effect of PA2-Vb. This new finding provides a new perspective on snake venom PLA_2

Please cite this article in press as: Zeng, F., et al. Crystal structure of phospholipase PA2-Vb, a protease-activated receptor agonist from the *Trimeresurus stejnegeri* snake venom. FEBS Lett. (2014), http://dx.doi.org/10.1016/j.febslet.2014.10.032

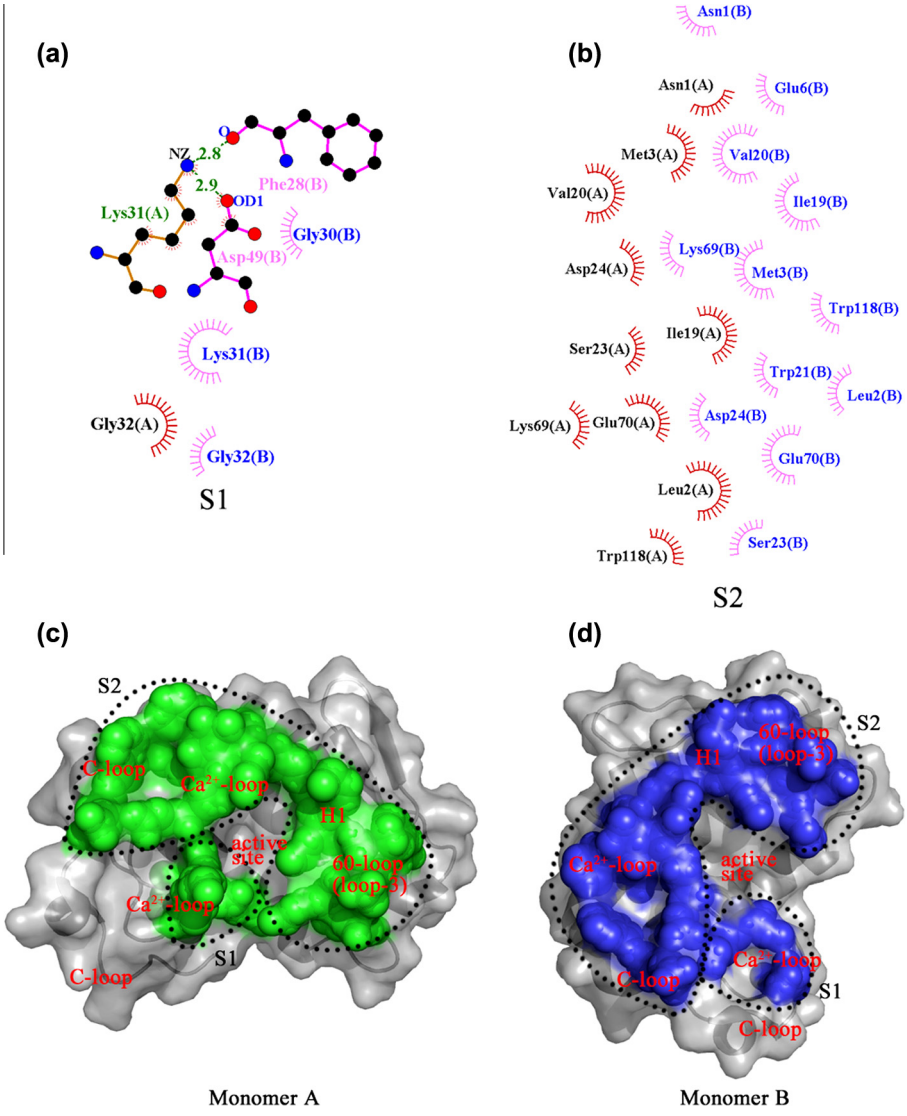

Fig. 7. The interface of the homodimer. (a and b) The S1 site and S2 site as shown by LigPlot^{+} software. (c and d) The interface shown in monomer (a) A and monomer (b) B.

function. Moreover, this function of PA2-Vb to activate PAR-1 represents a previously unknown function in svPLA$_2$.

Because PA2-Vb is an enzyme, the protease inhibitor *p*BPB was introduced to explore the relationship between its vasoconstriction activity and its enzymatic activity. In most svPLA$_2$s, the pharmacological effects such as antibacterial and antiparasitic actions are related to the products of hydrolysis [32]. But other activities of svPLA$_2$s were independent of their enzymatic activities. For example, the treatment with *p*BPB strongly reduced the bactericidal effect and partially decreased the neurotoxic effect of the PLA$_2$ from *Crotalus durissus collilineatus* venom [27]. In the present study, even though the chemical modification of His^{48} by *p*BPB in PA2-Vb could dramatically inhibit the catalytic activity of the enzyme, this modification did not affect the PA2-Vb effect on the vasoconstriction. This suggests that the vasoconstriction function of PA2-Vb is independent of its enzymatic activity.

Finally, the crystal structure of PA2-Vb was determined at a high resolution. It shows an overall fold typical of the PLA$_2$ family [1]. From gel filtration, both monomer and homodimer are observed in solution, which is consistent with the PISA prediction. Homodimer is usually found in svPLA$_2$ with different assembled conformations. In BthTX-II structure, the homodimer is assembled by its H1 α-helix, β-wing and Leu110 from C [5]. While, the acidic PLA$_2$ from the venom of Deinagkistrodon acutus uses i-face to stabilize the homodimer [9]. The oligomeric state is important for some PLA$_2$s [22]. In this study, the homodimer of PA2-Vb is also stabilized by the interaction between the i-face of the two molecules. The i-face of PLA$_2$ is a planar surface which surrounds the active site and binds to the phospholipid surface [35]. Previous studies have described that the i-faces of PLA$_2$s are structurally and functionally different than their active sites. The substrate accessibility of PLA$_2$s can be facilitated by the contact between the i-face and the interface of substrate. [29,35]. In PA2-Vb, the i-face consists of a patch of hydrophobic residues surrounded by polar residues and is involved in the binding of the phospholipid membrane. In addition, the Lys^{31} of monomer A is inserted into the active site of monomer B and forms several hydrogen bonds, which is consistent with the phospholipid binding model [2]. It is reported that PLA$_2$ first binds to the phospholipids membrane through its i-face. Then, with the assistance of polar residues that around the active sites, such as His48 or Lys69, the amphiphile head group inserts into the catalytic pocket, like the Lys^{31} of monomer A [33]. In PA2-Vb, four negative charged molecules, mapped as PEG molecules, bond to the positive charged pocket. In svPLA$_2$s,

Please cite this article in press as: Zeng, F., et al. Crystal structure of phospholipase PA2-Vb, a protease-activated receptor agonist from the *Trimeresurus stejnegeri* snake venom. FEBS Lett. (2014), http://dx.doi.org/10.1016/j.febslet.2014.10.032

this positive charged patch was usually made up of the conventional sequence: XBBBXXBX or XBBXBX in which B represents basic amino acid and X represents non-basic amino acids [6]. However, the function of this positive pocket is still unknown.

In summary, we successfully isolated and purified an acidic PLA_2 named PA2-Vb from *T. stejnegeri* venom, and characterized its vasoconstriction effect. Interestingly, we identify for the first time the molecular target of PA2-Vb in VSMCs, which acts on the PAR-1 receptor. We also uncovered the mechanism underlying the vasoconstriction through a PAR-1-PLCβ-IP_3R-Ca^{2+} release signaling pathway. Finally, we solved the PA2-Vb crystal structure at high resolution. Although it is unclear how PA2-Vb engages with the PAR-1 receptor, our work shads light on the relationship of animal toxins and Ca^{2+} homeostasis regulation.

Conflict of interest

The authors declare that they have no conflict of interest.

Acknowledgements

We thank the staff members in SSRF for the collection of diffraction data. This work was supported by the Fundamental Research Funds for the Central Universities; Chinese National Natural Science Foundation (Grant numbers: 81371284, 31130018, 30900224 and 10979039); Chinese Ministry of Science and Technology (Grant numbers: 2009CB825500 and 2012CB917200); Science and Technological Fund of Anhui Province for Outstanding Youth of China (Grant number: 10040606Y11); Anhui Provincial Natural Science Foundation of China (Grant number: 11040606M171 and 1108085J11).

Appendix A. Supplementary data

Supplementary data associated with this article can be found, in the online version, at http://dx.doi.org/10.1016/j.febslet.2014.10.032.

References

[1] Arni, R.K. and Ward, R.J. (1996) Phospholipase A_2 – a structural review. Toxicon 34 (8), 827–841.
[2] Bahnson, B.J. (2005) Structure, function and interfacial allosterism in phospholipase A_2: insight from the anion-assisted dimer. Arch. Biochem. Biophys. 433 (1), 96–106, http://dx.doi.org/10.1016/j.abb.2004.08.013.
[3] Balemba, O.B., Salter, M.J., Heppner, T.J., Bonev, A.D., Nelson, M.T. and Mawe, G.M. (2006) Spontaneous electrical rhythmicity and the role of the sarcoplasmic reticulum in the excitability of guinea pig gallbladder smooth muscle cells. Am. J. Physiol. Gastrointest. Liver Physiol. 290 (4), G655–G664, http://dx.doi.org/10.1152/ajpgi.00310.2005.
[4] Chen, V.B., Arendall 3rd, W.B., Headd, J.J., et al. (2010) MolProbity: all-atom structure validation for macromolecular crystallography. Acta Crystallogr. D Biol. Crystallogr. 66 (Pt 1), 12–21, http://dx.doi.org/10.1107/S0907444909042073.
[5] Correa, L.C., Marchi-Salvador, D.P., Cintra, A.C., Sampaio, S.V., Soares, A.M. and Fontes, M.R. (2008) Crystal structure of a myotoxic Asp49-phospholipase A_2 with low catalytic activity: insights into Ca^{2+}-independent catalytic mechanism. Biochim. Biophys. Acta 1784 (4), 591–599, http://dx.doi.org/10.1016/j.bbapap.2008.01.007.
[6] Delatorre, P., Rocha, B.A., Santi-Gadelha, T., Gadelha, C.A., Toyama, M.H. and Cavada, B.S. (2011) Crystal structure of Bn IV in complex with myristic acid: a Lys49 myotoxic phospholipase A(2) from *Bothrops neuwiedi* venom. Biochimie 93 (3), 513–518, http://dx.doi.org/10.1016/j.biochi.2010.11.003.
[7] Emsley, P. and Cowtan, K. (2004) Coot: model-building tools for molecular graphics. Acta Crystallogr. D Biol. Crystallogr. 60 (Pt 12 Pt 1), 2126–2132, http://dx.doi.org/10.1107/S0907444904019158.
[8] Gillespie, D. and Fill, M. (2008) Intracellular calcium release channels mediate their own countercurrent: the ryanodine receptor case study. Biophys. J . 95 (8), 3706–3714, http://dx.doi.org/10.1529/biophysj.108.131987.
[9] Gu, L., Zhang, H., Song, S., Zhou, Y. and Lin, Z. (2002) Structure of an acidic phospholipase A_2 from the venom of *Deinagkistrodon acutus*. Acta Crystallogr. D Biol. Crystallogr. 58 (Pt 1), 104–110.
[10] Han, S.K., Yoon, E.T., Scott, D.L., Sigler, P.B. and Cho, W. (1997) Structural aspects of interfacial adsorption. A crystallographic and site-directed mutagenesis study of the phospholipase A_2 from the venom of *Agkistrodon piscivorus piscivorus*. J. Biol. Chem. 272 (6), 3573–3582.
[11] Holm, L. and Rosenstrom, P. (2010) Dali server: conservation mapping in 3D. Nucleic Acids Res. 38 (Web Server issue), W545–W549, http://dx.doi.org/10.1093/nar/gkq366.
[12] Hu, P., Sun, L., Zhu, Z.Q., et al. (2008) Crystal structure of Natratoxin, a novel snake secreted phospholipaseA2 neurotoxin from Naja atra venom inhibiting A-type K+ currents. Proteins 72 (2), 673–683, http://dx.doi.org/10.1002/prot.21964.
[13] Joubert, F.J. and Taljaard, N. (1980) Purification, some properties and amino-acid sequences of two phospholipases A (CM-II and CM-III) from *Naja naja kaouthia* venom. Eur. J. Biochem./FEBS 112 (3), 493–499.
[14] Kini, R.M. (2003) Excitement ahead: structure, function and mechanism of snake venom phospholipase A_2 enzymes. Toxicon 42 (8), 827–840, http://dx.doi.org/10.1016/j.toxicon.2003.11.002.
[15] Kobayashi, S., Kitazawa, T., Somlyo, A.V. and Somlyo, A.P. (1989) Cytosolic heparin inhibits muscarinic and alpha-adrenergic Ca^{2+} release in smooth muscle. Physiological role of inositol 1,4,5-trisphosphate in pharmacomechanical coupling. J. Biol. Chem. 264 (30), 17997–18004.
[16] Laskowski, R.A., Macarthur, M.W., Moss, D.S. and Thornton, J.M. (1993) Procheck – a program to check the stereochemical quality of protein structures. J. Appl. Crystallogr. 26, 283–291, http://dx.doi.org/10.1107/S0021889892009944.
[17] Murshudov, G.N., Vagin, A.A. and Dodson, E.J. (1997) Refinement of macromolecular structures by the maximum-likelihood method. Acta Crystallogr. D Biol. Crystallogr. 53 (Pt 3), 240–255, http://dx.doi.org/10.1107/S0907444996012255.
[18] Otwinowski, Z. and Minor, W. (1997) Processing of X-ray diffraction data collected in oscillation mode. Methods Enzymol. 276, 307–326.
[19] Potterton, E., Briggs, P., Turkenburg, M. and Dodson, E. (2003) A graphical user interface to the CCP4 program suite. Acta Crystallogr. D Biol. Crystallogr. 59 (Pt 7), 1131–1137.
[20] Roberts, M.F., Deems, R.A., Mincey, T.C. and Dennis, E.A. (1977) Chemical modification of the histidine residue in phospholipase A_2 (*Naja naja naja*). A case of half-site reactivity. J. Biol. Chem. 252 (7), 2405–2411.
[21] Rouault, M., Rash, L.D., Escoubas, P., et al. (2006) Neurotoxicity and other pharmacological activities of the snake venom phospholipase A_2 OS2: the N-terminal region is more important than enzymatic activity. Biochemistry 45 (18), 5800–5816, http://dx.doi.org/10.1021/bi060217r.
[22] Ruller, R., Aragao, E.A., Chioato, L., et al. (2005) A predominant role for hydrogen bonding in the stability of the homodimer of bothropstoxin-I, A lysine 49-phospholipase A_2. Biochimie 87 (11), 993–1003, http://dx.doi.org/10.1016/j.biochi.2005.04.008.
[23] Salvador, G.H., Marchi-Salvador, D.P., Silveira, L.B., Soares, A.M. and Fontes, M.R. (2011) Crystallization and preliminary X-ray diffraction studies of BmooPLA2-I, a platelet-aggregation inhibitor and hypotensive phospholipase A_2 from *Bothrops moojeni* venom. Acta Crystallogr., Sect. F: Struct. Biol. Cryst. Commun. 67 (Pt 8), 900–902, http://dx.doi.org/10.1107/S174430911102392X.
[24] Searls, Y.M., Loganathan, R., Smirnova, I.V. and Stehno-Bittel, L. (2010) Intracellular Ca^{2+} regulating proteins in vascular smooth muscle cells are altered with type 1 diabetes due to the direct effects of hyperglycemia. Cardiovasc. Diabetol. 9, 8, http://dx.doi.org/10.1186/1475-2840-9-8.
[25] Shen, B., Cheng, K.T., Leung, Y.K., et al. (2008) Epinephrine-induced Ca^{2+} influx in vascular endothelial cells is mediated by CNGA2 channels. J. Mol. Cell. Cardiol. 45 (3), 437–445, http://dx.doi.org/10.1016/j.yjmcc.2008.06.005.
[26] Teixeira, S.S., Silveira, L.B., da Silva, F.M., et al. (2011) Molecular characterization of an acidic phospholipase A(2) from *Bothrops pirajai* snake venom: synthetic C-terminal peptide identifies its antiplatelet region. Arch. Toxicol. 85 (10), 1219–1233, http://dx.doi.org/10.1007/s00204-011-0665-6.
[27] Toyama, M.H., Toyama, D.O., Joazeiro, P.P., et al. (2005) Biological and structural characterization of a new PLA2 from the *Crotalus durissus collilineatus* venom. Protein. J. 24 (2), 103–112.
[28] Tsai, I.H., Wang, Y.M. and Hseu, M.J. (2011) Mutagenesis analyses explore residues responsible for the neurotoxic and anticoagulant activities of Trimucrotoxin, a pit-viper venom Asn6-phospholipase A_2. Biochimie 93 (2), 277–285, http://dx.doi.org/10.1016/j.biochi.2010.09.021.
[29] Tsai, Y.C., Yu, B.Z., Wang, Y.Z., Chen, J. and Jain, M.K. (2006) Desolvation map of the i-face of phospholipase A_2. Biochim. Biophys. Acta 1758 (5), 653–665, http://dx.doi.org/10.1016/j.bbamem.2006.04.003.
[30] Tsuboi, K., Sugimoto, Y. and Ichikawa, A. (2002) Prostanoid receptor subtypes. Prostaglandins Other Lipid Mediat. 68–69, 535–556.
[31] Vagin, A. and Teplyakov, A. (2000) An approach to multi-copy search in molecular replacement. Acta Crystallogr. D Biol. Crystallogr. 56 (Pt 12), 1622–1624.
[32] Vargas, L.J., Londono, M., Quintana, J.C., et al. (2012) An acidic phospholipase A with antibacterial activity from *Porthidium nasutum* snake venom. Comp. Biochem. Physiol. B: Biochem. Mol. Biol. 161 (4), 341–347 (doi: S1096-4959(12)00004-8 [pii] 10.1016/j.cbpb.2011.12.010).
[33] Wee, C.L., Balali-Mood, K., Gavaghan, D. and Sansom, M.S. (2008) The interaction of phospholipase A_2 with a phospholipid bilayer: coarse-grained molecular dynamics simulations. Biophys. J . 95 (4), 1649–1657, http://dx.doi.org/10.1529/biophysj.107.123190.

[34] Wei, J.F., Wei, X.L., Mo, Y.Z. and He, S.H. (2009) Induction of mast cell accumulation, histamine release and skin edema by N49 phospholipase A_2. BMC Immunol. 10, 21, http://dx.doi.org/10.1186/1471-2172-10-21.

[35] Winget, J.M., Pan, Y.H. and Bahnson, B.J. (2006) The interfacial binding surface of phospholipase A2s. Biochim. Biophys. Acta 1761 (11), 1260–1269, http://dx.doi.org/10.1016/j.bbalip.2006.08.002.

[36] Wray, S. and Burdyga, T. (2010) Sarcoplasmic reticulum function in smooth muscle. Physiol. Rev. 90 (1), 113–178, http://dx.doi.org/10.1152/physrev.00018.2008.

[37] Zeng, F., Shen, B., Zhu, Z., et al. (2013) Crystal structure and activating effect on RyRs of AhV_TL-I, a glycosylated thrombin-like enzyme from *Agkistrodon halys* snake venom. Arch. Toxicol. 87 (3), 535–545, http://dx.doi.org/10.1007/s00204-012-0957-5.

[38] Zeng, F., Zou, Z., Niu, L., Li, X. and Teng, M. (2013) AhV_aPA-induced vasoconstriction involves the IP(3)Rs-mediated Ca(2)(+) releasing. Toxicon 70, 107–113, http://dx.doi.org/10.1016/j.toxicon.2013.04.012.

[39] Zhang, P., Shi, J., Shen, B., et al. (2009) Stejnihagin, a novel snake metalloproteinase from Trimeresurus stejnegeri venom, inhibited L-type Ca^{2+} channels. Toxicon 53 (2), 309–315 (doi: S0041-0101(08)00610-7 [pii] 10.1016/j.toxicon.2008.12.006).

[40] Zhao, G., Adebiyi, A., Blaskova, E., Xi, Q. and Jaggar, J.H. (2008) Type 1 inositol 1,4,5-trisphosphate receptors mediate UTP-induced cation currents, Ca^{2+} signals, and vasoconstriction in cerebral arteries. Am. J. Physiol. Cell Physiol. 295 (5), C1376–C1384, http://dx.doi.org/10.1152/ajpcell.00362.2008.

Please cite this article in press as: Zeng, F., et al. Crystal structure of phospholipase PA2-Vb, a protease-activated receptor agonist from the *Trimeresurus stejnegeri* snake venom. FEBS Lett. (2014), http://dx.doi.org/10.1016/j.febslet.2014.10.032